Stability and vibrational properties of the hydrogen atom for p-type AlN doped with group-II: a first-principles study*

Zhang Jianmin(张健敏), Xu Guigui(许桂贵), Wu Qingyun(吴青云), Chen Zhigao(陈志高), and Huang Zhigao(黄志高)†

(Department of Physics, Fujian Normal University, Fuzhou 350007, China)

Abstract: The stability and local vibrational mode (LVM) of hydrogen related p-type AlN have been studied by first-principles calculations based on density functional theory. The stable and metastable microscopic geometries of group-II (Be, Mg, Ca, Sr, Ba)–H complexes have been investigated. The calculated results indicate that $BC_{\parallel}$ is the most stable configuration for isolated interstitial H^+ and Be–H complexes, while it is $AB_{N,\perp}$ for Mg–H, Ca–H, Sr–H and Ba–H complexes. Moreover, the vibrational frequencies and the values of k and $|\alpha|$ for the H atom with LVM are calculated. Here, the values of k and $|\alpha|$ are used to describe the parameters of the harmonic and anharmonic contributions, respectively. The calculated results indicate that the larger the size of the doped ion is, the shorter the N–H bond length is, and the larger the potential energy, the vibrational frequencies, the values of k and $|\alpha|$ are. This implies that the size of the doped ion has an important influence on the vibrational properties of H.

Key words: p-type AlN; local vibrational mode; group-II–H complexes; first-principles study
DOI: 10.1088/1674-4926/31/6/062001 **PACC:** 7280E; 6320

1. Introduction

Recently, the group-III nitrides and their alloys have drawn enormous attention as an essential and versatile class of semiconductor materials. Aluminum nitride (AlN) is an important semiconductor with a wide band gap (6.2 eV). It has attracted intense interest due to its novel properties and important applications. For example, it is a promising material in solid state lighting (light emitting diodes and laser diodes) from the visible to the deep-ultraviolet region of the spectrum[1–6], and it is also being attractively explored for applications in chemical sensors[7–9] and quantum cryptography[10] in the future. Due to its high ultrasonic velocity and fairly large electromechanical coupling coefficient, AlN is expected to become a thin-film piezoelectric material[11]. The low value of electron affinity (0.25 eV) of AlN is also interesting for applications of field emission devices at high power and temperature[12,13]. It is also potentially beneficial for electronic packaging applications due to its hardness, low coefficient of thermal expansion, and high thermal conductivity.

It is well known that hydrogen is abundantly present during the growth of AlN when NH_3 is used as a source gas in the usual preparation techniques, including metal-organic chemical vapor deposition (MOCVD), hydride vapor-phase epitaxy (HVPE) and molecular beam epitaxy (MBE). Hydrogen acting as a donor can passivate the dopants in p-type AlN, which results in deactivation of the acceptors[14,15]. Theoretical calculations indicate that the passivation is induced by the formation of electrical inactivation of dopant–H complexes[16]. Therefore, the detailed information about hydrogen (including the geometry and location of H) holds the key to optimizing the growth process and enhancing the acceptor concentrations. In experiment, infrared (IR) and Raman spectroscopy enable us to obtain the local vibrational modes (LVM) of hydrogen-related configurations. However, information on the interaction between hydrogen and shallow dopants in AlN can hardly be probed in experiment. Therefore, the theoretical calculation is crucial and helpful to explain the experimental facts. Although it has been reported that hydrogen prefers to incorporate with nitrogen in the group-III nitrides[17], the most favorable H site has not been identified when hydrogen is introduced into p-type AlN. Recently, AlN doped with group-II (such as Be-doped AlN[18], Mg:O codoped AlN[19], Ca-doped AlN[20]) was found to significantly improve the properties of p-type AlN. However, the various stable and metastable hydrogen-related configurations in p-type AlN doped with group-II (Be, Mg, Ca, Sr, Ba) have not been systemically investigated. In particular, the ion size effect of the hydrogen-related configurations has not been considered up to now. In this paper, the stable and metastable geometries of various hydrogen-related complexes (i.e., isolated H^+, Be–H, Mg–H, Ca–H, Sr–H, Ba–H) are studied based on total energy calculation. The frequencies of the H atom with anharmonic terms are calculated. Finally, the size effect on the stabilization and vibrational frequency is discussed.

2. Method

The geometry and vibrational frequencies of hydrogen related p-type AlN were studied by first-principles calculations. We employed the plane wave density functional theory

* Project supported by the National Key Project for Basic Research of China (No. 2005CB623605), the Fund of National Engineering Research Center for Optoelectronic Crystalline Materials (No. 2005DC105003), and the National Natural Science Foundation of China (No. 60876069).

† Corresponding author. Email: zghuang@fjnu.edu.cn

Received 2 September 2009, revised manuscript received 1 December 2009

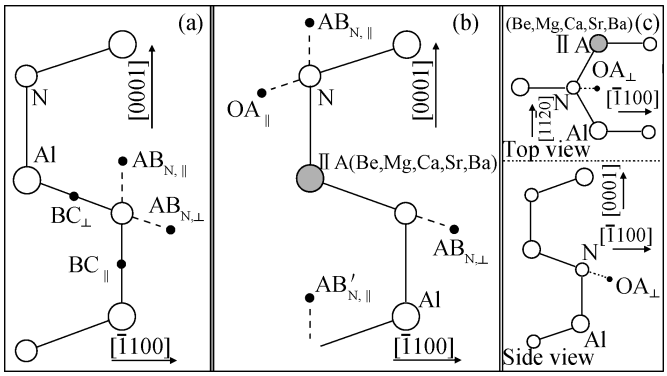

Fig. 1. Schematic illustration of possible hydrogen sites in the (11$\bar{2}$0) plane of wurtzite AlN. (a) Sites in bulk AlN. (b) Sites near the substitutional acceptors (Be, Mg, Ca, Sr, Ba). The large hollow circles, medium hollow circles, gray circles and small solid circles stand for Al atoms, N atoms, acceptors (Be, Mg, Ca, Sr or Ba) and possible sites for H, respectively. (c) $OA_\perp$ site.

(DFT)[21] in the local density approximation (LDA) with the Vanderbilt ultrasoft pseudopotentials[22] of exchange correlation, as implemented in the Vienna *ab-initio* simulation package (VASP)[23, 24]. The cutoff energy for the plane wave expansion of the electron wavefunction was set at 400 eV. A Γ-centered $3 \times 3 \times 3$ k mesh was adopted to sample the irreducible Brillouin zone for a $3 \times 3 \times 2$ supercell constructed from the structurally optimized AlN unit cell. Convergence tests indicated that these parameters ensured that the total energy was better than 1 meV. All atoms in each doped supercell were fully relaxed using the conjugate-gradient algorithm[25] until the maximum force on a single atom was less than 0.03 eV/Å.

All the calculations were performed for AlN with wurtzite structure. The lattice constants were chosen as follows: a = 3.08 Å and c = 4.94 Å, which are consistent with experimental values $a^{\exp}$ = 3.11 Å, $c^{\exp}$ = 4.98 Å. We then constructed the $3 \times 3 \times 2$ supercell geometry ($Al_{36}N_{36}$) containing 72 atoms with one Al atom replaced by a group-II (Be, Mg, Ca, Sr, Ba) atom, corresponding to a doped concentration of 2.78%. For the interstitial H, due to its light mass and strong N–H bond with positive charge state[14], the vibration mode of the N–H bond was considered. To investigate the vibrational stretching mode, candidate configurations for the dopant–H complexes have been established. A schematic illustration of these configurations is shown in Fig. 1. The AB_N (antibonding nitrogen) and BC (bond center) configurations have been previously studied for wurtzite structures[26]. There exist two types of configurations for AB_N and BC: one type is associated with bonds oriented parallel to the c axis with threefold symmetry, and typical sites are labeled as $BC_\parallel$ and $AB_{N,\parallel}$; the other type is associated with the bonds that are not parallel to the c axis. Although these are not exactly "perpendicular" to the c axis, the notations $BC_\perp$ and $AB_{N,\perp}$ are still used[27]. In addition, considering the possibility of H near to acceptors, Limpijumnong *et al*. proposed possible $OA_\parallel$, $OA_\perp$ and $AB'_{N,\parallel}$ configurations[28].

The oscillation potential of H, $V(x)$, can be described as follows:

$$V(x) = \frac{k}{2}x^2 + \alpha x^3 + \beta x^4, \tag{1}$$

where the coefficient of the quadratic term gives the harmonic frequency $\omega^0 = \sqrt{k/\mu}$, where the reduced mass μ is defined as: $\frac{1}{\mu} = \frac{1}{m_H} + \frac{1}{m_N}$, where m_H and m_N are the masses of the hydrogen and nitrogen atoms, respectively.

Higher order coefficients α and β describe anharmonic contributions. Moreover, the one-dimensional single-particle Schrödinger equation is described by

$$\left[-\frac{\hbar^2}{2\mu}\nabla^2 + V(x)\right]\psi(x) = E\psi(x). \tag{2}$$

Based on the perturbation theory[28, 29], an approximate analytical solution for the equation above can be obtained as follows:

$$\omega = \omega^0 + \Delta\omega = \sqrt{\frac{k}{\mu}} - 3\frac{\hbar}{\mu}\left[\frac{5}{2}\left(\frac{\alpha}{k}\right)^2 - \frac{\beta}{k}\right], \tag{3}$$

where ω is the total frequency, ω^0 is the harmonic frequency, and $\Delta\omega$ is the anharmonic contribution. The oscillation energies of H for given configurations can be calculated. In the calculation, H oscillates from its equilibrium site along the N–H or dopant–H bond directions. The oscillation frequencies can be obtained by fitting the potential energy curve $[V(x)$–$x]$.

3. Results and discussion

3.1. Energetics and structure of hydrogen-related configurations in p-type wurtzite AlN doped with Be, Mg, Ca, Sr, Ba atoms

The calculated total energy differences ΔE between various configurations of isolated H^+, Be(Mg, Ca, Sr, Ba)–H for AlN doped with group-II are listed in Table 1. For each case, the lowest energy configuration is chosen as a reference energy (0.00 eV). From the table, it is found that H with its stable charge state +1[26] prefers to stay at BC ($BC_\parallel$ and $BC_\perp$) sites, while energies at AB_N are slightly higher. In the process of relaxation, Al–N bonds are broken and a large amount of energy enables formation of the N–H bond, which is similar to the results for wurtzite GaN[28, 30]. Total energy calculations indicate that H favors the bond-center sites for AlN doped with Be, and $BC_\parallel$ is the stable state while $OA_\parallel$ is the metastable state with ΔE = 0.02 eV. This is attributed to the smaller size of beryllium than Al. Since the bond length of Be–N is smaller than that of Al–N, the N neighbors of Be are relaxed inwards. Therefore, H will readily turn to the most favorable state of $BC_\parallel$. However, it is observed that the $AB_{N,\perp}$ site is the most stable configuration for Mg–H, Ca–H, Sr–H and Ba–H complexes. Energies of the metastable configurations for Mg–H, Ca–H, Sr–H and Ba–H are 0.18, 0.62, 0.83, and 1.04 eV, respectively. In these cases, the sizes of the acceptor Mg, Ca, Sr and Ba atoms are larger than that of the Al atom, and therefore the dopant–N bond lengths are longer than the Al–N bond length. As a result, the N atoms surrounding the acceptor are pushed outwards, away from the dopant (Mg, Ca, Sr, Ba). In this case, H prefers to stay at the $AB_{N,\perp}$ site instead of BC positions. Moreover, the BC configurations are not even a metastable geometry. Figure 2 shows the total energies for all relevant structures in AlN doped with group-II. From the figure and Table 1, it is found that the total energies increase as the size of the doped ions increases. Moreover, it is noticed that when the size

Table 1. Calculated total energy differences ΔE (eV) between different candidate configurations of H in AlN doped with group-II. Values for isolated H^+ are included. We set the lowest energy configuration as a reference (set at 0.00 eV) in each case. The stable and metastable configurations are shown in boldface.

Configuration	H^+	Be–H	Mg–H	Ca–H	Sr–H	Ba–H
$BC_{\parallel}$	**0.00**	**0.00**	0.23	1.12	1.85	2.54
$BC_{\perp}$	**0.00**	0.06	0.34	0.83	0.96	1.06
$OA_{\parallel}$		**0.02**	0.20	0.76	1.21	1.64
$OA_{\perp}$		0.06	**0.18**	0.69	0.90	**1.04**
$AB_{N,\parallel}$	0.17	1.03	0.35	**0.62**	**0.83**	1.25
$AB_{N,\perp}$	0.03	0.67	0.00	**0.00**	**0.00**	**0.00**
$AB'_{N,\parallel}$		1.22	0.69	1.08	1.16	1.20

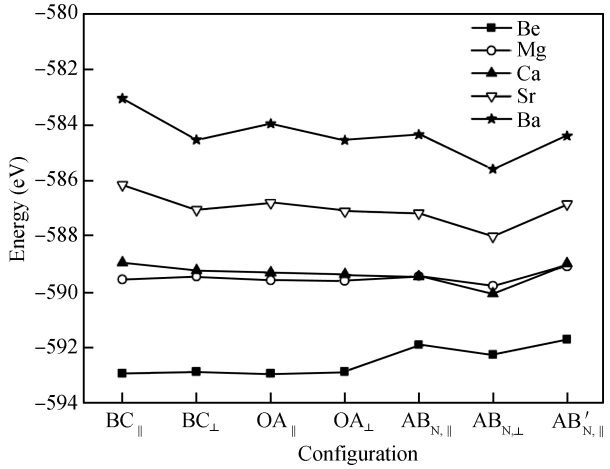

Fig. 2. Total energy of each configuration of H in p-type wurtzite AlN doped with group-II (Be, Mg, Ca, Sr, Ba).

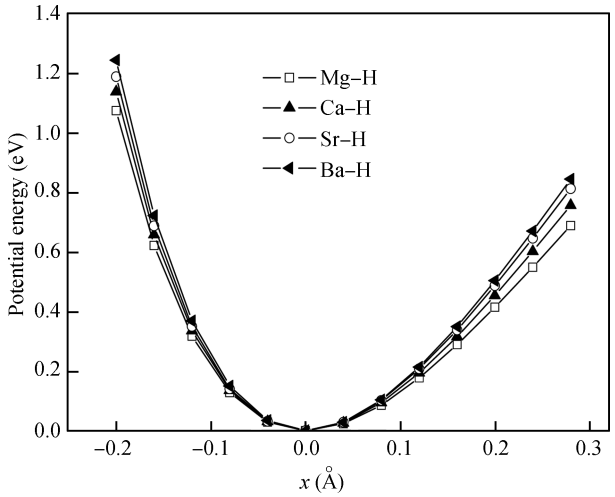

Fig. 3. Calculated potential energy as a function of N–H amplitude (x) for $AB_{N,\perp}$ configurations. The symbols represent the calculated points while the lines are traced to fit the fourth order polynomial based on Eq. (1). The potential energies are set to be zero at the equilibrium position for each structure.

of the acceptor grows, the energy difference between the stable and metastable configurations becomes sharply larger.

3.2. Vibrational frequencies for stretching modes

Calculated results of the vibration of N–H bond-stretching modes for all configurations of H^+ and AlN doped with group-II are listed in Table 2. The relaxed lengths of N–H bond d_{N-H}, the fitting parameters $k/2$, α, β for the fourth order polynomial potential, and frequencies including harmonic and anharmonic are obtained. From Table 2, it is found that H prefers to bond with the N atom inward of a sphere with a radius of approximately 1 Å, which is consistent with the results of hydrogen-related GaN[30].

In the previous test calculations, the symmetric stretch-mode frequency of NH_3 has been found to be 3280 cm^{-1}[28] and 3194 cm^{-1}[31]. This is 57 and 143 cm^{-1} smaller than the experimental value of 3337 cm^{-1}[32], respectively. We get an average frequency (including anharmonic terms) of 3180 cm^{-1} for N–H, which is consistent with 3194 cm^{-1}[31]. The calculated frequencies for the stable configurations of H^+, Be–H, Mg–H, Ca–H, Sr–H, Ba–H in AlN are listed in Table 3. In comparison with the results above, those for the stable configurations of H^+, Be–H, Mg–H in GaN, and the estimated frequencies on the basis of the N–H bond length with ω^0 = 3860 – 16164 (d_{N-H} – 1.000), ω = 3768 – 20790 (d_{N-H} – 1.000), are also listed in Table 3. From the table, it is found that the relative stable positions and the vibrational frequencies of the H atom for H^+, Be–H, Mg–H are quite similar to those in GaN. Moreover, the calculated frequencies are consistent with the theoretically estimated values based on the correlated equation between vibrational frequencies and N–H bond length.

The calculated results above indicate that the vibrational frequencies of H at $BC_{\parallel}$ are higher than those at any other positions. Its most limited space and exactly parallel orientation to the c axis strengthen the N–H bonds and increase the vibrational frequencies. Moreover, it is found that the vibrational frequencies for the $BC_{\parallel}$ configuration increase with increasing size of the doped ion. The highest vibrational frequency is 4476 cm^{-1} for Ba–H and the lowest value is 3340 cm^{-1} for Be–H. We then focus on the $AB_{N,\perp}$ site, which is the most stable configuration for Mg–H, Ca–H, Sr–H and Ba–H. Figure 3 shows the calculated potential energy as a function of N–H amplitude (x) for $AB_{N,\perp}$configurations of Mg–H, Ca–H, Sr–H, Ba–H. From the figure, it is found that the potential energy for the Ba–H complex is the largest, while that for the Mg–H complex is the smallest. The calculated N–H bond length (d_{N-H}) and vibrational frequencies with harmonic frequencies and anharmonic contributions are shown in Fig. 4, respectively. From the figure, it is found that the vibrational frequencies increase with decreasing N–H bond length (d_{N-H}).

The parameter k determines the values of the harmonic frequencies based on $\omega^0 = \sqrt{k/\mu}$, while α describes the anhar-

Table 2. Calculated relative formation energies, N–H bond distance (d_{N-H}), and vibrational properties with N–H bond-stretching modes for H^+ and Be(Mg, Ca, Sr, Ba)–H. $k/2$, α, and β are the second, third, and fourth order coefficients in the polynomial of Eq. (1), in eV/Å^n, where n is the order of the coefficient. ω is the total vibrational frequency: $\omega = \omega^0 + \Delta\omega$, where ω^0 and $\Delta\omega$ are the harmonic and anharmonic components of the frequency. All frequencies are in cm^{-1}.

Type	Configuration	ΔE (eV)	d_{N-H} (Å)	$k/2$	α	β	ω^0	$\Delta\omega$	ω
H^+	$BC_{\parallel}$	0.00	1.024	22.27	−46.74	51.28	3587	−143	3444
H^+	$BC_{\perp}$	0.00	1.028	21.04	−45.56	51.26	3486	−153	3333
H^+	$AB_{N,\perp}$	0.03	1.056	15.70	−40.11	45.60	3011	−235	2777
H^+	$AB_{N,\parallel}$	0.17	1.046	17.40	−42.01	50.24	3180	−196	2984
Be–H	$BC_{\parallel}$	0.00	1.029	21.11	−45.67	51.96	3492	−151	3340
Be–H	$OA_{\parallel}$	0.02	1.029	20.93	−45.09	51.53	3477	−149	3328
Be–H	$BC_{\perp}$	0.06	1.025	21.67	−47.05	54.09	3537	−152	3386
Be–H	$OA_{\perp}$	0.06	1.030	20.31	−45.58	50.23	3425	−170	3255
Be–H	$AB_{N,\perp}$	0.67	1.054	14.66	−41.11	96.59	2910	−145	2765
Be–H	$AB_{N,\parallel}$	1.03	1.042	19.16	−41.37	49.58	3327	−144	3182
Be–H	$AB'_{N,\parallel}$	1.22	1.072	13.55	−36.33	41.93	2797	−263	2534
Mg–H	$AB_{N,\perp}$	0.00	1.051	16.80	−41.28	45.90	3115	−215	2900
Mg–H	$OA_{\perp}$	0.18	1.052	15.81	−41.59	44.14	3022	−261	2760
Mg–H	$OA_{\parallel}$	0.20	1.032	20.04	−45.54	46.70	3402	−184	3218
Mg–H	$BC_{\parallel}$	0.23	1.017	23.73	−47.81	55.04	3702	−123	3579
Mg–H	$BC_{\perp}$	0.34	1.038	17.92	−44.61	46.33	3217	−230	2986
Mg–H	$AB_{N,\parallel}$	0.35	1.039	19.11	−41.85	48.15	3322	−155	3167
Mg–H	$AB'_{N,\parallel}$	0.69	1.054	16.45	−39.30	44.85	3082	−197	2886
Ca–H	$AB_{N,\perp}$	0.00	1.043	17.96	−42.74	47.28	3221	−198	3022
Ca–H	$AB_{N,\parallel}$	0.62	1.032	20.33	−44.06	53.24	3427	−145	3282
Ca–H	$OA_{\perp}$	0.69	1.047	16.46	−42.98	47.53	3083	−251	2832
Ca–H	$OA_{\parallel}$	0.76	1.038	18.32	−44.86	49.90	3253	−213	3040
Ca–H	$BC_{\perp}$	0.83	1.034	18.02	−46.20	50.29	3226	−242	2984
Ca–H	$AB'_{N,\parallel}$	1.08	1.049	18.22	−39.31	47.02	3244	−145	3099
Ca–H	$BC_{\parallel}$	1.12	1.000	20.99	−45.70	53.37	3482	−151	3331
Sr–H	$AB_{N,\perp}$	0.00	1.037	18.99	−43.76	46.89	3312	−186	3126
Sr–H	$AB_{N,\parallel}$	0.83	1.021	22.31	−46.47	56.89	3589	−128	3461
Sr–H	$OA_{\perp}$	0.90	1.040	17.56	−44.85	48.98	3185	−239	2945
Sr–H	$BC_{\perp}$	0.96	1.031	18.60	−46.52	49.82	3277	−229	3048
Sr–H	$AB'_{N,\parallel}$	1.16	1.042	19.31	−41.20	49.09	3340	−140	3199
Sr–H	$OA_{\parallel}$	1.21	1.039	17.88	−43.80	48.29	3213	−214	2999
Sr–H	$BC_{\parallel}$	1.85	0.981	32.57	−54.42	71.36	4337	−58	4279
Ba–H	$AB_{N,\perp}$	0.00	1.031	19.75	−46.27	51.41	3377	−190	3187
Ba–H	$OA_{\perp}$	1.04	1.037	18.03	−45.13	49.97	3227	−226	3002
Ba–H	$BC_{\perp}$	1.06	1.033	17.92	−46.81	51.99	3217	−251	2966
Ba–H	$AB'_{N,\parallel}$	1.20	1.040	19.65	−41.31	48.06	3369	−137	3232
Ba–H	$AB_{N,\parallel}$	1.25	1.003	25.99	−51.06	65.27	3874	−103	3771
Ba–H	$OA_{\parallel}$	1.64	1.048	16.40	−41.93	47.34	3078	−236	2842
Ba–H	$BC_{\parallel}$	2.54	0.973	35.54	−56.54	68.89	4531	−55	4476

Table 3. Calculated N–H bond lengths and vibrational frequencies for stable configurations of all the complexes mentioned.

Type	Stable configuration	d_{N-H} (Å)		ω^0 (cm^{-1})			Ω (cm^{-1})		
		This work	Ref. [28][a]	This work	Ref. [28][a]	Theory[b]	This work	Ref. [28][a]	Theory[b]
H^+	$BC_{\parallel}$	1.024	1.027	3587	3581	3472	3444	3453	3269
Be–H	$BC_{\parallel}$	1.029	1.028	3492	3478	3391	3340	3299	3165
Mg–H	$AB_{N,\perp}$	1.051	1.031	3115	3333	3036	2900	3045	2707
Ca–H	$AB_{N,\perp}$	1.043		3221		3164	3022		2874
Sr–H	$AB_{N,\perp}$	1.037		3312		3262	3126		2999
Ba–H	$AB_{N,\perp}$	1.031		3377		3359	3187		3124

[a] Results for H^+, Be–H and Mg–H in wurtzite GaN in Ref. [28].
[b] Obtained with the equations $\omega^0 = 3860 - 16164\ (d_{N-H})$, $\omega = 3768 - 20790\ (d_{N-H})$, as found in Ref. [28].

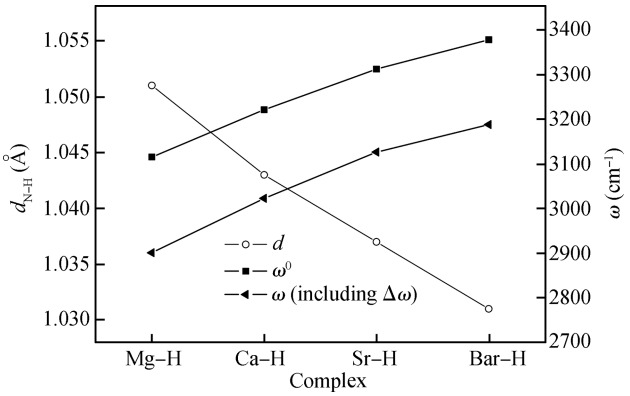

Fig. 4. Relaxed N–H bond length (d_{N-H}) and vibrational frequencies (ω) for $AB_{N,\perp}$ configurations of Mg–H, Ca–H, Sr–H, Ba–H. Square symbols indicate harmonic frequencies and triangle symbols indicate frequencies including anharmonic contributions.

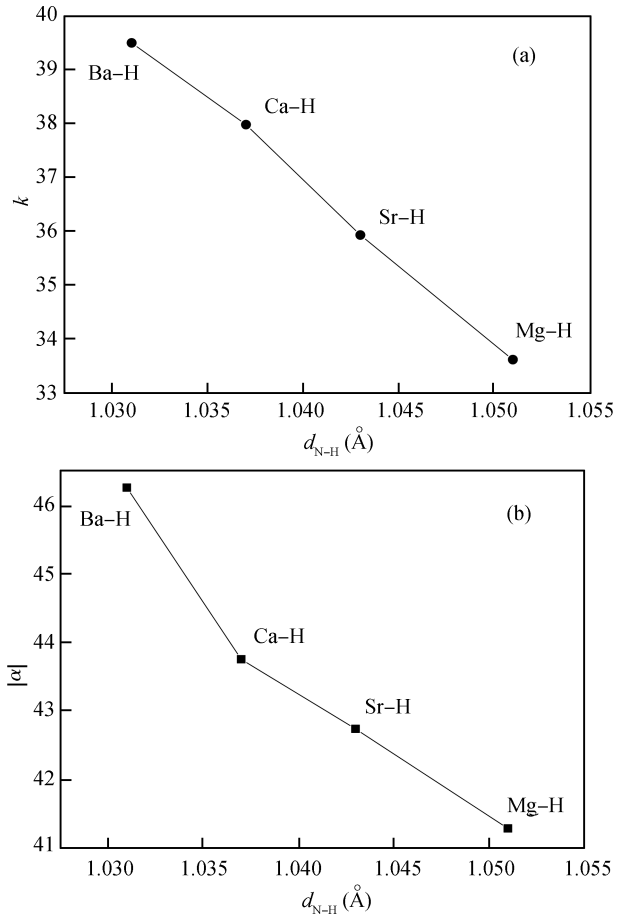

Fig. 5. Polynomial coefficients (a) k and (b) $|\alpha|$ as a function of relaxed N–H bond length (d_{N-H}) for $AB_{N,\perp}$ configurations of Mg–H, Ca–H, Sr–H, Ba–H.

monic contributions. From Table 2, it is found that the values of k and $|\alpha|$ for Be–H with a longer N–H bond length are smaller than those for Al–H (i.e., H^+), which is because the ion size of Be is smaller than that of Al. A similar size effect exists in Mg–H, Ca–H, Sr–H, Ba–H. Figure 5 shows the values of k and $|\alpha|$ as a function of relaxed N–H bond length (d_{N-H}) for $AB_{N,\perp}$ configurations of Mg–H, Ca–H, Sr–H, Ba–H. From the figure, it is found the values of k and $|\alpha|$ decrease with increasing N–H bond length, or with decreasing size of the doped ion. From the discussion above, it is found that the larger the size of doped ion is, the shorter the N–H bond length is, and the larger the potential energy, vibrational frequencies, and values of k and $|\alpha|$ are. This means that the size of the doped ion has an important influence on the vibrational properties of H.

4. Conclusions

In conclusion, we have studied the microscopic geometry and vibrational properties for hydrogen in different p-type AlN doped with Be, Mg, Ca, Sr and Ba. The calculated results of total energies suggest that H prefers to bind to N, forming a stable N–H complex. Moreover, it is found that $BC_{\parallel}$ is the most stable configuration for isolated interstitial H^+ and Be–H complexes, while it is $AB_{N,\perp}$ for Mg–H, Ca–H, Sr–H and Ba–H complexes. The vibrational frequencies for the H atom with LVM in these complexes are also calculated. The calculated results indicate that the larger the size of doped ion, the shorter the N–H bond length is, and the larger the potential energy, vibrational frequencies, and values of k and $|\alpha|$ are. It is considered that the size of the doped ion has an important influence on the vibrational properties of H.

References

[1] Vurgaftman I, Meyer J R, Ram-Mohan L R. Band parameters for III–V compound semiconductors and their alloys. J Appl Phys, 2001, 89: 5815

[2] Vurgaftman I, Meyer J R. Band parameters for nitrogen-containing semiconductors. J Appl Phys, 2003, 94: 3675

[3] Nam K B, Li J, Lin J Y, et al. Deep ultraviolet picosecond time-resolved photoluminescence studies of AlN epilayers. Appl Phys Lett, 2003, 82: 1694

[4] Chiu W Y, Wu C H, Kao H L, et al. The optical properties and applications of AlN thin films prepared by a helicon sputtering system. J Vac Sci Technol A, 2002, 20: 843

[5] Yu Y, Ren T L, Liu L T. High quality silicon-based AlN thin films for MEMS application. Integrated Ferroelectrics, 2005, 69: 367

[6] Benetti M, Cannata D, Di Pietrantonio F, et al. Growth of AlN piezoelectric film on diamond for high-frequency surface acoustic wave devices. IEEE Trans Ultrason Ferroelectr Freq Control, 2005, 52: 1806

[7] Stutzmann M, Steinhoff G, Eickhoff M, et al. GaN-based heterostructures for sensor applications. Diamond Related Materials, 2002, 11: 886

[8] Schalwig J, Müller G, Eickhoff M, et al. Group III-nitride-based gas sensors for combustion monitoring. Mater Sci Eng B, 2002, 93: 207

[9] Lu H, Schaff W J, Eastman L F. Surface chemical modification of InN for sensor applications. J Appl Phys, 2004, 96: 3577

[10] Kako S, Santori C, Hoshino K, et al. A galliumnitride single-photon source operating at 200 K. Nature Mater, 2006, 5: 887

[11] Kubota K, Kobayashi Y, Fujimoto K. Preparation and properties of III–V nitride thin films. J Appl Phys, 1989, 66: 2984

[12] Benjamin M C, Wang C, Davis R F, et al. Observation of a negative electron affinity for heteroepitaxial AlN on alpha(6H)-SiC(0001). Appl Phys Lett, 1994, 64: 3288

[13] Wu Y F, Keller B P, Keller S, et al. Very high breakdown voltage and large transconductance realized on GaN heterojunction field effect transistors. Appl Phys Lett, 1996, 69: 1438

[14] Van de Walle C G, Neugebauer J. Universal alignment of hydrogen levels in semiconductors, insulators and solutions. Nature, 2003, 423: 626
[15] Pankove J I, Johnson N M. Hydrogen in semiconductors. In: Semiconductors and semimetals. Vol. 34. San Diego: Academic Press, 1991
[16] Limpijumnong S, van de Walle C G. Passivation and doping due to hydrogen in III-nitrides. Phys Status Solidi B, 2001, 228: 303
[17] Du M H, Limpijumnong S, Zhang S B. Hydrogen-mediated nitrogen clustering in dilute III–V nitrides. Phys Rev Lett, 2006, 97: 075503
[18] Wu R Q, Shen L, Yang M. Possible efficient p-type doping of AlN using Be: an *ab initio* study. Appl Phys Lett, 2007, 91: 152110
[19] Wu R Q, Shen L, Yang M. Enhancing hole concentration in AlN by Mg:O codoping: *ab initi*o study. Phys Rev B, 2008, 77: 073203
[20] Zhang Y, Liu W, Liang P. Half-metallic ferromagnetism in Ca-doped AlN from first-principles study. Solid State Commun, 2008, 147: 254
[21] Kohn W, Sham L J. Self-consistent equations including exchange and correlation effects. Phys Rev, 1965, 140: A1133
[22] Vanderbilt D. Soft self-consistent pseudopotentials in a generalized eigenvalue formalism. Phys Rev B, 1990, 41: 7892
[23] Kresse G, Hafner J. *Ab initio* molecular dynamics for open-shell transition metals. Phys Rev B, 1993, 48: 13115
[24] Kresse G, Furthmuller J. Efficiency of ab-initio total energy calculations for metals and semiconductors using a plane-wave basis set. Comput Mater Sci, 1996, 6: 15
[25] Xu G G, Wu Q Y, Chen Z G, et al. Disorder and surface effects on work function of Ni–Pt metal gates. Phys Rev B, 2008, 78: 115420
[26] Myers S M, Wright A F, Petersen G A, et al. Equilibrium state of hydrogen in gallium nitride: theory and experiment. J Appl Phys, 2000, 88: 4676
[27] Limpijumnong S, Northrup J E, van de Walle C G. Entropy-driven stabilization of a novel configuration for acceptor-hydrogen complexes in GaN. Phys Rev Lett, 2001, 87: 205505
[28] Limpijumnong S, Northrup J E, van de Walle C G. Identification of hydrogen configurations in p-type GaN through first-principles calculations of vibrational frequencies. Phys Rev B, 2003, 68: 075206
[29] Landau L D, Lifshitz E M. Quantum mechanics. 3rd ed. Oxford: Pergamon Press, 1977
[30] Neugebauer J, van de Walle C G. Hydrogen in GaN: novel aspects of a common impurity. Phys Rev Lett, 1995, 75: 4452
[31] Li X, Keyes B, Asher S, et al. Hydrogen passivation effect in nitrogen-doped ZnO thin films. Appl Phys Lett, 2005, 86: 122107
[32] Nickel N H, McCluskey M D, Zhang S B. Hydrogen in semiconductors. Pittsburgh: Materials Research Society, 2004